

# Catalytic performance of chloromethane transformation for light olefins production over SAPO-34 with different Si content

Yingxu Wei,<sup>a,b</sup> Dazhi Zhang,<sup>a</sup> Yanli He,<sup>a</sup> Lei Xu,<sup>a</sup> Yue Yang,<sup>a</sup> Bao-Lian Su,<sup>b</sup> and Zhongmin Liu<sup>a,\*</sup>

<sup>a</sup>Applied Catalysis Laboratory, Dalian Institute of Chemical Physics, Chinese Academy of Sciences, P.O. Box 110, Dalian 116023, P.R. China

<sup>b</sup>Laboratoire de Chimie des Matériaux Inorganiques, ISIS, The University of Namur (FUNDP), 61 rue de Bruxelles, Namur B-5000, Belgium

Received 15 November 2006; accepted 17 January 2007

SAPO-34s with low and high Si content were synthesized and characterized by XRD, XRF, NMR, FTIR and TG-DSC. Different Si content generated no apparent difference in XRD patterns and <sup>31</sup>P and <sup>27</sup>Al MAS NMR spectra. The Si coordination states studied by <sup>29</sup>Si MAS NMR predicted the acidity difference caused by Si incorporation. The absorbance of bridge hydroxyls in FTIR spectra also showed the amount of active sites differed with Si content. Both of the two samples were employed as catalysts in the transformation of chloromethane to light olefins and proved to be very selective catalysts for light olefins production. The influences of Si content on chloromethane conversion and product selectivity were investigated in details. Coke amount and coke species were determined by TG-DSC and FTIR. Coke formation was related to the Si content of SAPO-34 and corresponded to the catalytic performance.

**KEY WORDS:** chloromethane; light olefins; SAPO-34; Si incorporation.

## 1. Introduction

Light olefins, ethylene and propylene, are the most important chemicals among petrochemical products. The main commercial technique for their production is steam cracking of naphtha at high temperature (800–880 °C), which is known as the first energy-consuming process in petrochemical industry. With the sharp increase of the price of crude oil and growing need of light olefins, the development of alternative routes for light olefins production attracts much interest from academia and industry. The most successful process developed until now is MTO, starting from methane via syngas and methanol as intermediates [1,2]. For further rational and efficient utilization of natural gas for higher hydrocarbons production, some research efforts were also put on some other possible routes, such as catalytic conversion of methane through halogenated methane intermediates.

In 1985, Olah and co-workers described a very interesting three-steps catalytic process for the transformation of methane to higher hydrocarbons through monohalogenation of methane, hydrolysis of halide methane to methanol, and then the MTG reaction on HZSM-5 [3]. In 1988, Taylor et al. invented a cyclic process on the basis of their research for the production of gasoline from methane with chloromethane as the intermediate [4]. Compared with the work of Olah et al.,

the transformation from methane to gasoline was reduced to two stages, i.e. the oxyhydrochlorination (OHC) for production of CH<sub>3</sub>Cl from methane, and MTG for directly transferring methyl chloride to gasoline. In the second stage, HCl generated as by-product and could be recycled for the first step. This is a quite innovative process and applicable in industry. In the following study of chloromethane transformation [5–9], ZSM-5 appeared to be the most promising catalyst due to their high activity and long life in the reaction and a strong reduction in the coke formation. In the most of the work with ZSM-5 as catalyst, higher hydrocarbons, such as alkanes and aromatics in gasoline range, were the main products. Compared with the extensive study in MTO field, the work on the selective transformation of chloromethane to light olefins was quite limited. Y. Sun and coworkers found P or P and Mg modification for ZSM-5 could improve light olefins production in chloromethane conversion [10].

A large series of work was carried out on zeolite catalysts, while SAPO-type molecular sieves application in chloromethane transformation was less reported. SAPO-34, a microporous SAPO molecular sieve with CHA structures, has been a very selective catalyst for light olefins production from methanol due to its moderate acidity and small pore opening [2,11]. In our very recent study, SAPO-34 and metal-substituted SAPO-34 was employed as catalysts in chloromethane transformation and presented excellent catalytic performance [12–14], especially for the production of light olefins from chloromethane conversion. The work of S. Svelle

\*To whom correspondence should be addressed.  
E-mail: Liuzm@dicp.ac.cn

et al. also proves the high olefins selectivity and structural stability of SAPO-34 in the conversion of chloromethane to olefins [15].

For SAPO molecular sieves, Si incorporation into AlPO framework is the key for the acid site generation and correspondent acid-catalyzing reaction [15–18]. When SAPO-34 is used in the chloromethane transformation, it is also interesting to find variable catalytic performance with different Si incorporation. So in the present study, two SAPO-34 samples with high and low Si content were synthesized and their framework element coordination states, surface acidity, and catalytic performance were compared and investigated to address the effect of the Si content of SAPO-34 on the chloromethane conversion, product selectivity and coke formation.

## 2. Experimental

### 2.1. Synthesis

SAPO-34 was prepared with hydrothermal method [19,20] following the procedure in our previous study [13,14]. The chemical composition of the starting gel was  $1.0\text{Al}_2\text{O}_3:1.0\text{P}_2\text{O}_5:0.2\text{SiO}_2:3.0\text{TEA}:50\text{H}_2\text{O}$  and  $1.0\text{Al}_2\text{O}_3:1.0\text{P}_2\text{O}_5:0.8\text{SiO}_2:3.0\text{TEA}:50\text{H}_2\text{O}$  for the samples with low and high Si content. The gels were sealed in the stainless-steel autoclaves lined with polytetrafluoroethylene (PTFE). The autoclaves containing the gels were heated at  $200\text{ }^\circ\text{C}$  for 24 h under autogenetic pressure. The products were filtrated, washed, and dried at  $110\text{ }^\circ\text{C}$  for 3 h. The obtained samples with high and low Si content were denoted as SAPO-34 (HS) and SAPO-34 (LS) respectively.

### 2.2. Characterization

The crystallinity and the phase purity of the as-synthesized samples were analyzed by powder X-ray diffraction (RIGAKU D/max-rb powder diffractometer) with  $\text{CuK}\alpha$  radiation. The chemical composition of the samples was determined with Bruker SRS-3400 XRF spectrometer.  $^{31}\text{P}$ ,  $^{27}\text{Al}$  and  $^{29}\text{Si}$  MAS NMR spectra were recorded on a Bruker DRX-500 NMR spectrometer. The surface hydroxyls were tested with FTIR. Self-supported SAPO-34 wafers ( $15\text{ mg/cm}^2$ ) were first calcined in a flow of dry oxygen at  $450\text{ }^\circ\text{C}$  for 10 h and then in vacuum for 4 h. After cooling to room temperature, the spectra of SAPO-34 phase were recorded using a Bruker EQUINOX 55 spectrometer.

### 2.3. Chloromethane conversion

#### 2.3.1. Catalytic performance

The catalytic tests were performed using a fixed bed reactor system at atmosphere pressure. 0.62 g of catalyst was loaded into a quartz reactor with an inner diameter of 5 mm. The sample was pretreated in a flow of dry

nitrogen at  $500\text{ }^\circ\text{C}$  for 1 h and then the temperature of reactor was adjusted to  $450\text{ }^\circ\text{C}$  and the atmosphere was replaced by nitrogen and chloromethane (the molar ratio of  $\text{N}_2/\text{CH}_3\text{Cl}$  was 1). The weight hourly space velocity (WHSV) was  $3.2\text{ h}^{-1}$  for chloromethane. The product stream was kept at  $180\text{ }^\circ\text{C}$  and analyzed on-line by a Varian GC3800 gas chromatograph equipped with a FID detector and a PONA capillary column.

#### 2.3.2. Coke formation studied by thermal analysis and FTIR

The coke deposition of the catalysts after reaction was analyzed by TG-DSC method. An amount of 10–15 mg of discharged catalyst was loaded in the crucible of the microbalance. The temperature was increased from room temperature to  $800\text{ }^\circ\text{C}$  at a rate of  $10\text{ }^\circ\text{C}/\text{min}$  under dry air flow. The weight loss and calorimetric effect were recorded.

The discharged catalysts were mixed with KBr and compressed. The IR spectra of the wafer were recorded with a Bruker EQUINOX 55 spectrometer with  $4\text{ cm}^{-1}$  resolution.

## 3. Results and discussion

### 3.1. Synthesis

The X-ray diffraction patterns of the two as-synthesized molecular sieves are presented in figure 1. They are in agreement with that of SAPO-34 reported in the literature [20]. No obvious difference in X-ray diffraction and peak intensity is observed between the two samples. The chemical composition of the calcined samples was determined by XRF and listed in Table 1. The ratio of  $(\text{Si}+\text{P})/\text{Al}$  is 1 for SAPO-34(LS) and 1.04 for SAPO-34(HS), indicating that Si incorporation may occur in different way.

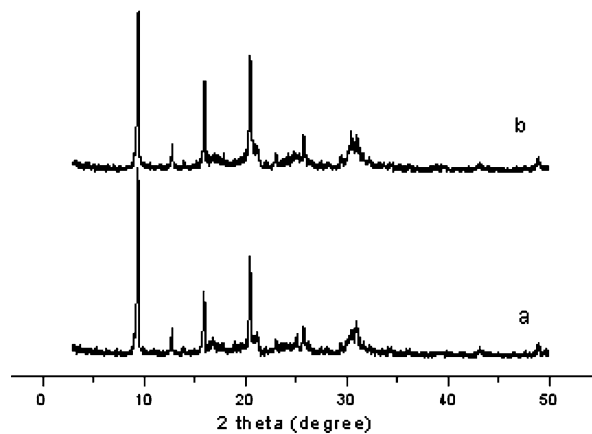


Figure 1. XRD patterns of the as-synthesized samples, (a) SAPO-34(LS) (b) SAPO-34(HS).

Table 1  
Molar composition of the synthesized sample

Product	Mole composition	(Si + P)/Al
SAPO-34(LS)	$\text{Al}_{0.50}\text{P}_{0.44}\text{Si}_{0.06}\text{O}_2$	1.00
SAPO-34(HS)	$\text{Al}_{0.49}\text{P}_{0.41}\text{Si}_{0.10}\text{O}_2$	1.04

### 3.2. $^{31}\text{P}$ , $^{27}\text{Al}$ and $^{29}\text{Si}$ MAS NMR spectra

The two samples with different Si content gave very similar  $^{31}\text{P}$  and  $^{27}\text{Al}$  MAS NMR spectra, so they are not given in the present study. The signal at  $-29$  ppm, due to typical P(4Al) species in AIPO and SAPO framework [18], presented in  $^{31}\text{P}$  MAS NMR spectra. In  $^{27}\text{Al}$  MAS NMR spectra, the two signals at 39 ppm and 8 ppm, assigned to tetrahedrally coordinated framework Al atoms and Al atom of higher coordination states respectively, were observed for both samples studied. Previous reports have associated the signal at 7.7 ppm with pentacoordinated Al atoms formed by the additional coordination of one water to tetrahedrally coordinated Al species [21].

$^{29}\text{Si}$  MAS NMR spectra in figure 2 show that the synthesized SAPO-34 sample with low Si content just gives one signal with the chemical shift of  $-91$  ppm, representing that just one Si coordination state, Si(4Al), appears in the framework. For SAPO-34 (HS), with more Si incorporation, beside the signal of Si(4Al) with high intensity, Si(3Al) coordination state with chemical shift of  $-95$  ppm could be clearly distinguished and Si( $n$ Al) signals ( $n = 2, 1, 0$ ) at  $-100$ ,  $-105$  and  $-110$  ppm also appear with very low intensity. It is known that Si atoms incorporate into the  $\text{AlPO}_4$  framework by two substitution mechanisms [15–17].

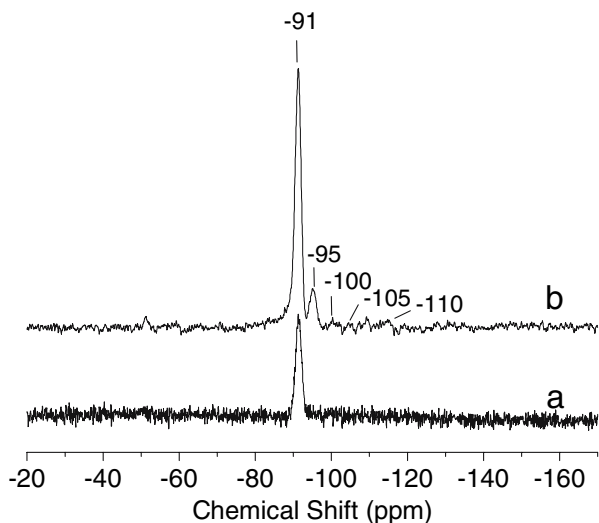


Figure 2.  $^{29}\text{Si}$  MAS NMR spectra of SAPO-34 (LS)-a and SAPO-34 (HS)-b.

One mechanism (SM2) is that one Si substitution for one P to form Si(4Al) entities, which gives rise to negatively charged framework and relatively weak Brönsted acid sites. On the other hand, the double substitution of neighboring Al and P by two Si atoms (SM3) to form Si( $n$ Al) ( $n = 3-0$ ) structures leads to the formation of stronger Brönsted acid sites. From the final composition of synthesized samples in Table 2, the ratio of Si + P/Al is 1 for SAPO-34 (LS) and 1.04 for SAPO-34 (HS), indicating that Si incorporation of SAPO-34 (LS) follows SM2, and both SM2 and SM3 substitution may occur during the synthesis of SAPO-34 (HS). The acidic strength of bridge hydroxyl species of Si( $n$ Al) follows the order of Si(1Al) > Si(2Al) > Si(3Al) > Si(4Al) [16], so from the Si spectra, with more Si incorporation, beside the increase of acid amount of SAPO-34, the acid strength may also change. SAPO-34(HS) may have more acid sites and stronger acidity than SAPO-34(LS).

### 3.3. Surface hydroxyls studied by FTIR

Figure 3 gives the FTIR spectra of activated SAPO-34s with high and low Si content. Both of the two spectra present four peaks in the range of  $4000-3000\text{ cm}^{-1}$ . Two peaks at  $3675$  and  $3743\text{ cm}^{-1}$ , with low intensity, are assigned to P-OH and Si-OH, respectively, which are generated at the defect sites of SAPO-34 surface. The other two peaks at  $3625$  and  $3600\text{ cm}^{-1}$  can be attributed to two types of Si(OH)Al groups differed in their localization. The bridged hydroxyls at  $3600\text{ cm}^{-1}$  is assumed to be localized in the hexagonal prism, forming an H-bond with adjacent oxygen atoms of the framework while the isolated bridged OH groups pointing towards the center of the elliptical cages give

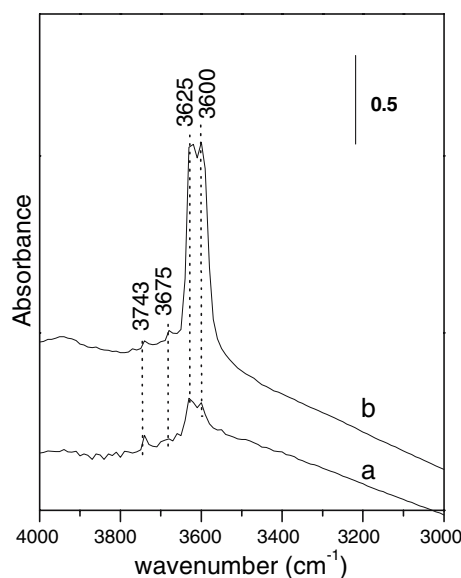


Figure 3. FTIR spectra of activated SAPO-34 (LS)-a and SAPO-34 (HS)-b.

the vibration frequency at  $3625\text{ cm}^{-1}$  [22–23]. These two types of OH groups are considered to be the active sites for acid-catalyzing reaction [24,25]. Stronger absorbance at  $3625$  and  $3600\text{ cm}^{-1}$  indicates higher intensity of bridge hydroxyls. More Si incorporation gives rise to the generation of more surface Brönsted acid sites.

### 3.4. Chloromethane transformation over SAPO-34s

#### 3.4.1. Catalytic performance

Chloromethane transformation was carried out over SAPO-34 with high and low Si content and the results of conversion and product selectivity are given in Figs. 4–6. The conversion evolution as a function of reaction time depicted in figure 4 shows that during the transformation, the chloromethane conversion over SAPO-34(HS) is higher than that over SAPO-34 (LS), indicating that the sample with higher Si content is more active than the lower one. At the reaction time of 5 min, the conversion is 98% for the SAPO-34(HS), while the value is just 47% for SAPO-34(LS). With prolonged reaction time, the conversion decreases for both of the samples. The catalysts may lose part of the activity with chloromethane transformation.

Figure 5 gives the products distribution in carbon number at the reaction time of 65 min. It is quite interesting to observe that  $C_2$  and  $C_3$  hydrocarbons are the main products of this reaction catalyzed by SAPO-34. This is significantly different from the products obtained on a series of large pore zeolite catalysts, such as X, Y, EMT, Beta, MOR and medium pore zeolite ZSM-5 [3–10] and should be attributed to the 8-ring pore opening of SAPO-34. The narrow pore opening favors the production of light hydrocarbons and sterically hinders the migration of larger hydrocarbon molecules, such as aromatic and hydrocarbons higher than  $C_6$ , even they may form in the cages. For the two samples, the difference of product selectivity caused by Si content is not very remarkable,  $C_2$  and  $C_3$  products as

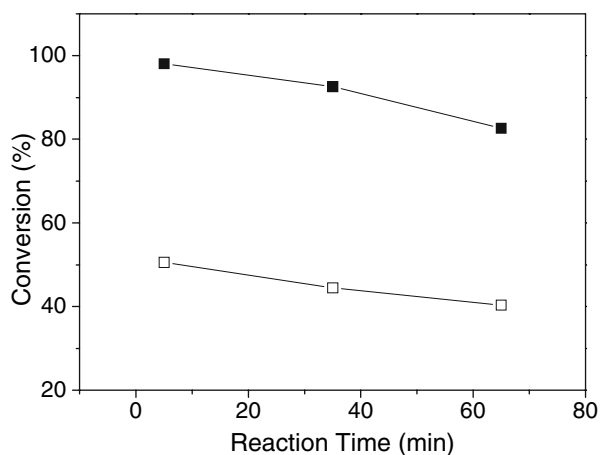


Figure 4. Chloromethane conversion over SAPO-34 (LS)-□ and SAPO-34 (HS)-■ with reaction time ( $T = 450\text{ }^{\circ}\text{C}$ ).

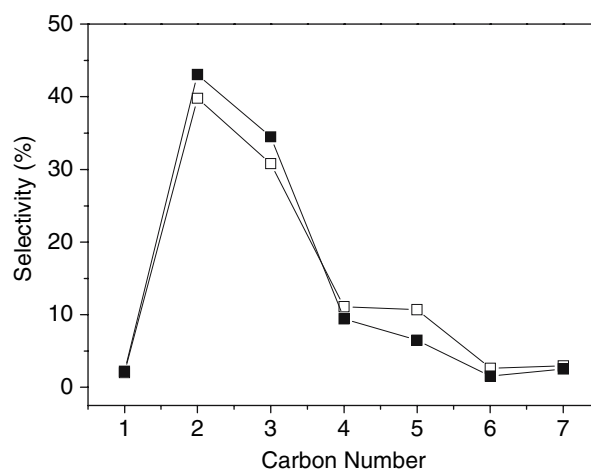


Figure 5. Product distribution in carbon number of chloromethane conversion over SAPO-34 (LS)-□ and SAPO-34 (HS)-■ ( $T = 450\text{ }^{\circ}\text{C}$ , Reaction time = 65 min).

the main for the two samples, but it can still be found clearly that more Si incorporation favors the generation of smaller products. In fact, the formation of  $C_2$  and  $C_3$  products over SAPO-34(HS) is more predominant than SAPO-34 (LS), while relatively more  $C_4$  and hydrocarbons larger than  $C_4$  appear among the products in SAPO-34(LS)-catalyzed reaction.

Group composition of the products at reaction time of 65 min is detailed in figure 6. Among the products, light alkenes, such as ethylene, propylene and butenes predominate. Detailed alkene distribution of the two samples (figure 6-a) indicates that higher ethylene selectivity appears over SAPO-34(HS) than SAPO-34(LS), while the selectivities of propylene and butenes over SAPO-34(HS) are slightly lower. This is consistent of the result of carbon number distribution. With the formation of large amount of light alkenes as the main products, relatively small amount of light alkanes are observed. It is easy to find that the selectivity of ethane, propane and butane over SAPO-34(HS) is higher than SAPO-34(LS). The ratio of  $C_3^0/C_3^=$ , defined as hydrogen transfer index (HTI), is used to evaluate the hydrogen transfer level. High HTI value means secondary reaction of alkene products on SAPO-34(HS), such as hydrogen transfer reaction is more readily to occur than SAPO-34(LS). Correspondingly, more alkanes and aromatic products may generate. Because only trace of aromatic products appear in the products stream, which is caused by the sterical hinderance of the 8-member ring pore opening of SAPO-34, relatively high selectivity of alkane predicts the deposition of H-unsaturated species. More coke may form over the surface of catalyst SAPO-34(HS). In SAPO-34(LS), just Si(4Al) presents in the framework. Isolation of acid sites is responsible for the low alkane formation from alkene oligomerization and followed hydrogen-transfer reaction. During the reaction, HCl is also observed in the

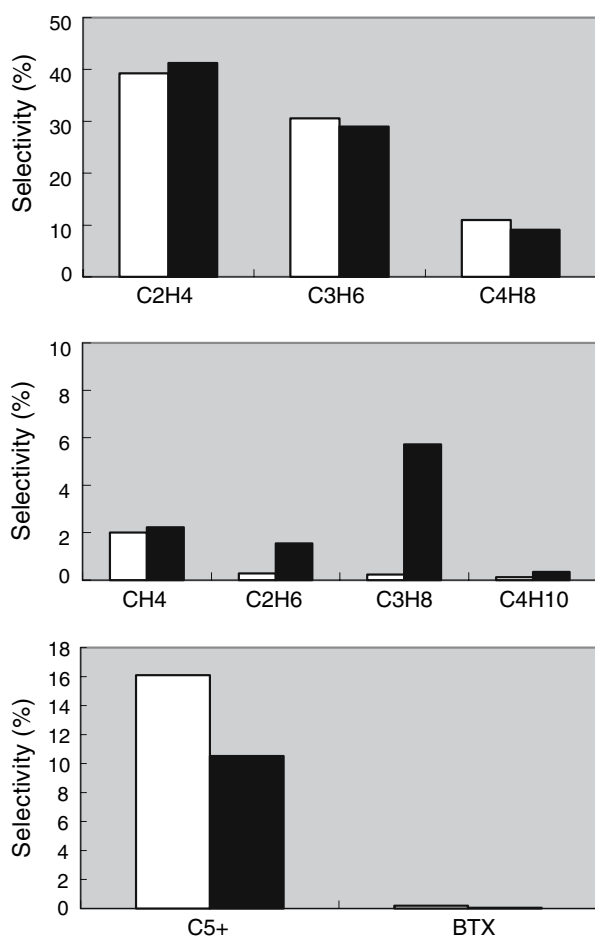


Figure 6. Product selectivity of chloromethane transformation over SAPO-34 (LS)-□ and SAPO-34 (HS)-■ ( $T = 450\text{ }^{\circ}\text{C}$ , Reaction time = 65 min).

products and its component is not listed in the product distribution.

### 3.4.2. Coke formation studied by TG-DSC and FTIR

Catalyst deactivation due to coke formation has been observed in MTO process over SAPO-34 [26]. In the present study, the deactivation of SAPO-34 catalyst also occurs during chloromethane transformation. Conversion decrease with reaction time shown in figure 4 stems from the coke formation over catalyst surface. Coke deposition of the discharged catalyst SAPO-34(HS) and SAPO-34(LS) was analyzed by TG-DSC and the results are given in figure 7.

TG analysis (figure 7A) shows two weight losses (I and II) in the range of 25–800  $^{\circ}\text{C}$ . The first weight loss (I) with endothermic effect (figure 7B) in the range of 25–200  $^{\circ}\text{C}$  is attributed to water desorption. The second weight loss (II) in the range of 200–550  $^{\circ}\text{C}$ , accompanied by exothermic effect, corresponds to the coke removal. For two SAPO-34s, the combustion of the coke species occurs in the same temperature range, while the weight loss value from coke removal is different. The weight loss from coke removal of SAPO-34(HS) is 9.9 wt%,

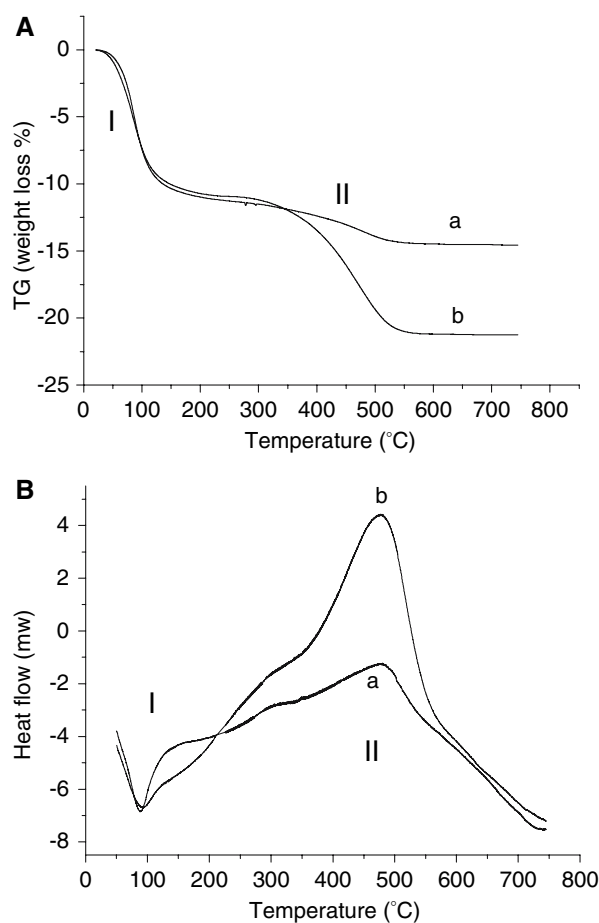


Figure 7. Thermal analysis (TG-A and DSC-B) of discharged catalysts SAPO-34(LS)-a and SAPO-34(HS)-b after reaction at 450  $^{\circ}\text{C}$  for 65 min.

while this value is 3.3 wt% for SAPO-34(LS). Catalysts lose their activity with coke deposition. The conversion decreases from 98% to 80%, and from 55 to 40% for SAPO-34(HS) and SAPO-34(LS) respectively. For SAPO-34(HS), its higher HTI value caused by relative strong acidity from Si(nAl) ( $n = 3-0$ ) species results in relatively large amount of alkanes production. Coke formation, usually from the oligomerization of light alkenes and followed H-transfer reaction, may also accelerate for this reason.

The FTIR spectra of the discharged catalysts SAPO-34(LS) and SAPO-34(HS) were given in figure 8. The broad bands centered at 1615  $\text{cm}^{-1}$  from SAPO-34(LS) in figure 8-a and 1632  $\text{cm}^{-1}$  from SAPO-34(HS) in figure 8-b should be attributed to adsorbed water, which have been tested in TG-DSC analysis. Beside this band, three distinct bands can be observed in the spectrum of SAPO-34(HS) (figure 8-b). The band at 1572  $\text{cm}^{-1}$  ascribed to C–C stretching vibration of hydrogen-deficient aromatic hydrocarbon species and the other two bands at 1382 and 1445  $\text{cm}^{-1}$  due to C–H deformation vibration predict the coke species deposition. However, these three absorbances are not clearly present in the

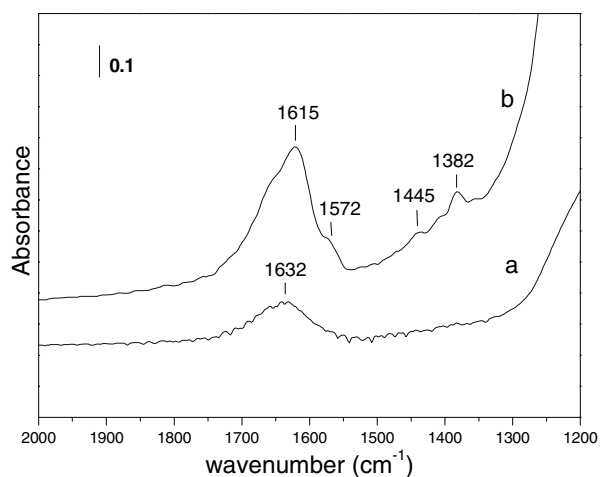


Figure 8. FTIR analysis of discharged catalysts SAPO-34(LS)-a and SAPO-34(HS)-b after reaction at 450 °C for 65 min.

spectrum of SAPO-34(LS) in figure 8-a, because of low coke amount over the SAPO-34 catalyst with low Si content.

Coke formation correlates with the strength and density of acid sites over the catalyst surface. The  $^{29}\text{Si}$  MAS NMR spectra (figure 2) and FTIR spectra (figure 3) indicate that more Si incorporation brings about stronger and dense bridge hydroxyls over SAPO-34(HS) surface as active sites, which are responsible for the fast transformation of chloromethane and more coke deposition. The primary hydrocarbons generation during induction period of MTO process remains controversial [27,28], while olefins assembly on the unsaturated and cyclic carbonaceous reaction center is known as the dominating route in the steady state of methanol reaction. Our previous study employed hydrocarbon-pool mechanism to explain the chloromethane conversion to higher hydrocarbons [13]. In the present study, the higher conversion on SAPO-34(HS) could be due to the relatively rich hydrogen-deficient species deposition in the cage of SAPO-34. These coke species could be the organic reaction center for light olefins generation, as have been found in MTO process by mass spectra and NMR techniques [29–31].

#### 4. Conclusion

The correlations between Si content of SAPO-34 with framework element coordination, acidity and catalytic performance were investigated. Si(4Al) is the only coordination state of SAPO-34 with low Si content. With more Si incorporation, beside Si(4Al) coordination state, Si( $n$ Al) ( $n = 3-0$ ) also appear in the  $^{29}\text{Si}$  MAS NMR spectra, predicting the stronger acidity. FTIR proves that more Si incorporation gives rise to more bridge hydroxyl groups as surface Brönsted acid sites. Both of the SAPO-34 catalysts with low and high

Si content are very selective catalysts for light olefins production from chloromethane transformation. Higher chloromethane conversion and higher ethylene selectivity were obtained over SAPO-34(HS). Less Si incorporation into SAPO-34(LS) favors the propylene production and reduces coke deposition. Hydrogen-deficient hydrocarbon species form in the cage of SAPO-34 catalyst, which may behave as the reaction centers for olefin production from chloromethane conversion.

#### References

- [1] C.D. Chang, *Catal. Rev. Sci. Eng.* 25(1) (1983) 1.
- [2] C.D. Chang, *Catal. Rev. Sci. Eng.* 26(3/4) (1984) 323.
- [3] G.A. Olah, B. Gupta, M. Farina, J.D. Felberg, W.M. Ip, A. Husain, R. Karpeles, K. Lammertsma, A.K. Melhotra and N.J. Trivedi, *J. Am. Chem. Soc.* 107 (1985) 7097.
- [4] C.E. Taylor and R.P. Noceti, *Stud. Surf. Sci. Catal.* 36 (1988) 483.
- [5] C.E. Taylor, R.R. Anderson, J.R. D'Este and R.P. Noceti, *Stud. Surf. Sci. Catal.* 130 (2000) 3633.
- [6] P. Lersch and F. Bändermann, *Appl. Catal.* 75 (1991) 133.
- [7] D. Jaumain and B.L. Su, *Stud. Surf. Sci. Catal.* 130 (2000) 1607.
- [8] D. Jaumain and B.L. Su, *J. Mol. Catal. A: Chemical* 197 (2003) 263.
- [9] D.K. Murray, T. Howard, P.W. Goguen, T.R. Krawietz and J.F. Haw, *J. Am. Chem. Soc.* 116 (1994) 6354.
- [10] Y. Sun, S.M. Campbell, J.H. Lunsford, G.E. Lewis, D. Palke and L.-M. Tau, *J. Catal.* 143 (1993) 32.
- [11] J. Liang, H.Y. Li, S.Q. Zhao, W.G. Guo, R.H. Wang and M.L. Ying, *Appl. Catal.* 64 (1990) 31.
- [12] Y. Wei, D. Zhang, L. Xu, Z. Liu and B.-L. Su, *Catal. Today* 106 (2005) 84.
- [13] Y. Wei, D. Zhang, Z. Liu and B.-L. Su, *J. Catal.* 238 (2006) 46.
- [14] Y. Wei, Y. He, D. Zhang, L. Xu, S. Meng, Z. Liu and B.-L. Su, *Micropor. Mesopor. Mater.* 90 (2006) 188.
- [15] S. Svelle, S. Aravinthan, M. Bjørgen, K.-P. Lillerud, S. Kolboe, I.M. Dahl and U. Olsbye, *J. Catal.* 241 (2006) 243.
- [16] R.B. Borade and A. Clearfield, *J. Mol. Catal.* 88 (1994) 249.
- [17] A.M. Prakash and S. Unnikrishnan, *J. Chem. Soc., Faraday Trans.* 90 (1994) 2291.
- [18] S. Ashtekar, S.V.V. Chilukuri and D.K. Chakrabarty, *J. Phys. Chem.* 98 (1994) 4878.
- [19] B.M. Lok, C.A. Messina, R.L. Patton, R.T. Gajek, T.R. Cannan and E.M. Flanigen, *J. Am. Chem. Soc.* 106 (1984) 6092.
- [20] B.M. Lok, C.A. Messina, R.L. Patton, R.T. Gajek, T.R. Cannan and E.M. Flanigen, *US Patent No. 4, 440, 871* (1984).
- [21] A. Buchholz, W. Wang, M. Xu, A. Arnold and M. Hunger, *Micropor. Mesopor. Mater.* 56 (2002) 267.
- [22] S.A. Zubkov, L.M. Kustov, V.B. Kazansky, I. Girnus and R. Fricke, *J. Chem. Soc. Faraday Trans.* 87 (1991) 897.
- [23] Y. Jeanvoine, J.G. Angyan, G. Kresse and J. Hafner, *J. Phys. Chem. B* 102 (1998) 5573.
- [24] L. Smith, A.K. Cheetham, R.E. Morris, L. Marchese, J.M. Thomas and P.A. Wright, *J. Chem. Sci.* 271 (1996) 799.
- [25] L. Smith, A.K. Cheetham, L. Marchese, J.M. Thomas, P.A. Wright, J. Chen and E. Gianotti, *Catal. Lett.* 41 (1996) 13.
- [26] D. Chen, K. Moljord, T. Fuglerud and A. Holmen, *Micropor. Mesopor. Mater.* 29 (1999) 191.
- [27] J.F. Haw, D.M. Marcus and P.W. Kletnieks, *J. Catal.* 244 (2006) 130.
- [28] Y. Jiang, W. Wang, V.R.R. Marthala, J. Huang, B. Sulikowski and M. Hunger, *J. Catal.* 244 (2006) 134.
- [29] H. Fu, W. Song and J.F. Haw, *Catal. Lett.* 76 (2001) 89.
- [30] B. Arstad and S. Kolboe, *Catal. Lett.* 71 (2001) 209.
- [31] B. Arstad and S. Kolboe, *J. Am. Chem. Soc.* 123 (2001) 8137.